Table 1 - The seasonal trends in the success of detecting *Morella* invasion, expressed as the Kappa coefficient, for the different unmixing approaches. The number of bands used in the analysis (n°) are also indicated. Kappa results are shown for the optimal or maximal Kappa. In between parantheses the MESMA classification threshold at which the highest Kappa was achieved is given.

	MESMA		**SZU**		**uSZU$_{0.001}$**		**uSZU$_{0.005}$**		**uSZU$_{0.01}$**		**SZU$_{0.005}$**		**uSZU$_{fixed}$**	
	Kappa	*n°*	*Kappa*	*n°*	*Kappa*	*n°*	*Kappa*	*n°*	*Kappa*	*n°*	*Kappa*	*n°*	*Kappa*	*n°*
January	0.66 (46)	117	0.66 (49)	86	0.73 (42)	36	0.60 (46)	23	0.70 (45)	15	0.60 (43)	23	0.60 (39)	35
March	0.51 (45)	117	0.56 (45)	88	0.53 (48)	41	0.59 (45)	19	0.54 (42)	13	0.55 (46)	19	0.52 (48)	30
July	0.69 (38)	117	0.73 (30)	74	0.72 (33)	32	0.73 (31)	15	0.71 (39)	10	0.65 (34)	15	0.65 (38)	12
August	0.66 (30)	117	0.70 (20)	63	0.73 (29)	34	0.73 (23)	12	0.73 (26)	9	0.69 (24)	12	0.72 (23)	14
September	0.69 (31)	117	0.73 (28)	90	0.67 (28)	45	0.75 (23)	21	0.72 (31)	14	0.69 (26)	21	0.69 (31)	27
October	0.53 (52)	117	0.61 (52)	105	0.62 (41)	32	0.69 (31)	13	0.66 (34)	8	0.60 (36)	13	0.62 (40)	11

Table 2 - The success of detecting *Morella* invasion, expressed as the Kappa coefficient, through multi-temporal unmixing. Results are shown for different scenarios drawing upon a different set of available images and for the different unmixing algorithms. The number of bands used in the analysis (n°) are also indicated. Kappa results are shown for the optimal or maximal Kappa. In between parantheses the MESMA classification threshold at which the highest Kappa was achieved is given.

	Scenario	**MESMA**		**SZU**		**$uSZU_{0.001}$**		**$uSZU_{0.005}$**		**$uSZU_{0.01}$**		**$SZU_{0.005}$**		**$uSZU_{fixed}$**	
		Kappa	*n°*	*Kappa*	*n°*	*Kappa*	*n°*	*Kappa*	*n°*	*Kappa*	*n°*	*Kappa*	*n°*	*Kappa*	*n°*
I	Jan, Mar, Jul, Aug, Sep, Oct	0.73 (34)	702	0.73 (35)	544	0.76 (36)	105	0.75 (28)	36	0.78 (26)	23	0.74 (29)	37	0.69 (23)	37
II	Jan, Mar, Aug, Sep, Oct	0.72 (36)	585	0.76 (39)	458	0.74 (44)	96	0.75 (25)	35	0.78 (26)	22	0.73 (21)	35	0.72 (25)	35
III	Jan, Mar, Aug, Oct	0.72 (39)	468	0.72 (37)	354	0.73 (31)	82	0.75 (22)	34	0.78 (39)	21	0.73 (21)	34	0.73 (22)	34
IV	Jan, Mar, Oct	0.54 (51)	351	0.54 (43)	262	0.56 (38)	80	0.75 (44)	31	0.66 (46)	19	0.53 (39)	31	0.53 (44)	31
V	Mar, Oct	0.40 (51)	234	0.48 (50)	172	0.58 (46)	58	0.59 (41)	25	0.60 (46)	15	0.53 (39)	25	0.48 (47)	27

Figure 1 – (left) Overview of the Hawaii Volcanoes National Park on the Island of Hawaii (imagery from the Carnegie Airborne Observatory; Asner et al., 2008a); (right) detail of the native ohia (*Metrosideros*) forests. Although most of this area is under protection by the U.S. National Park Service, it has experienced a number of biological invasions predominantly by *Morella faya* (from Somers & Asner, 2012a). The black box indicates the area covered by the Hyperion images.

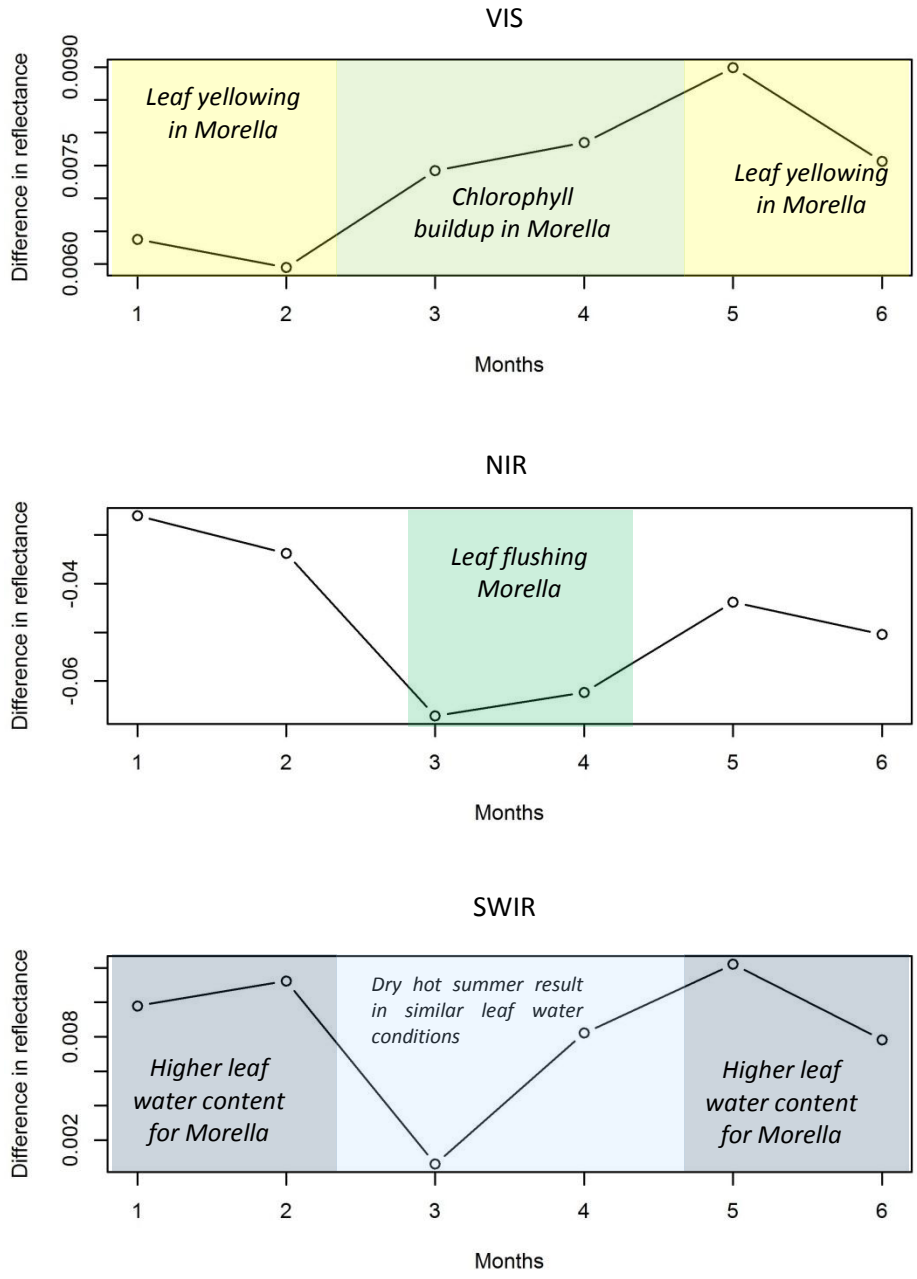

Figure 2 – Illustration of the linkage between ground phenology and the mean difference in Hyperion reflectance between *Metrosideros* and *Morella*. Results are shown for: VIS (400-700 nm), NIR (800-1300 nm), and SWIR (1500-1700 nm) reflectance (supported by Asner et al. 2006, Somers & Asner, 2012a,b, 2013).

Spectral Endmember Libraries

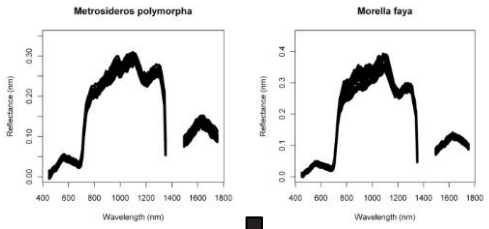

Calculate Spectral Correlation Matrix

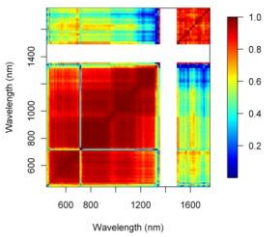

Calculate SI spectrum and select the band with highest SI (🟢)

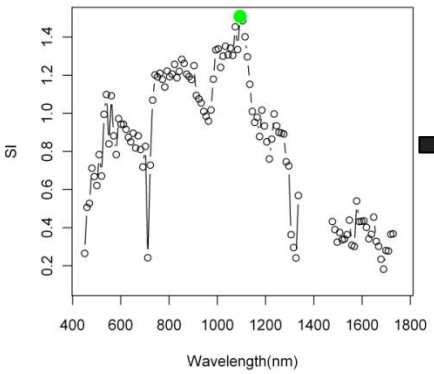

Remove all bands displaying a correlation > c (e.g. 0.99) with the selected band (-)

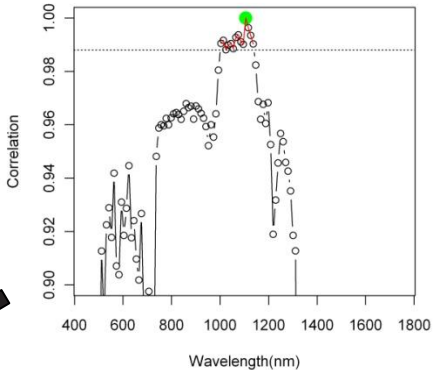

Select a second band as the one with the highest SI in the remaining band set (🟢)

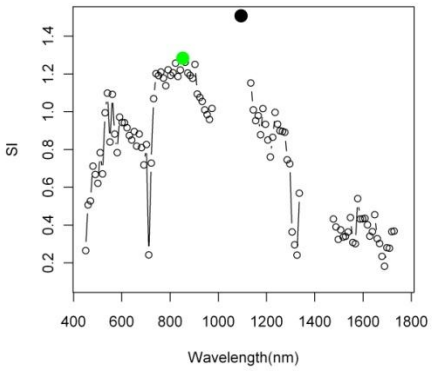

Remove all bands displaying a correlation > c-i with the selected band (-). In this illustration i is set to 0.01.

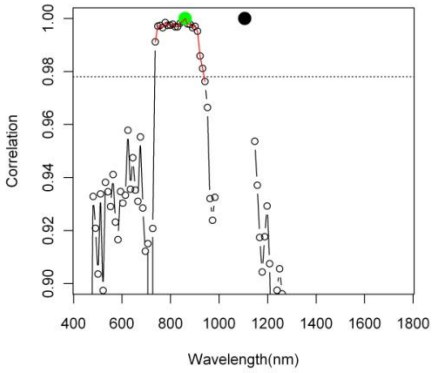

Select a third band as the one with the highest SI in the remaining band set (🟢)

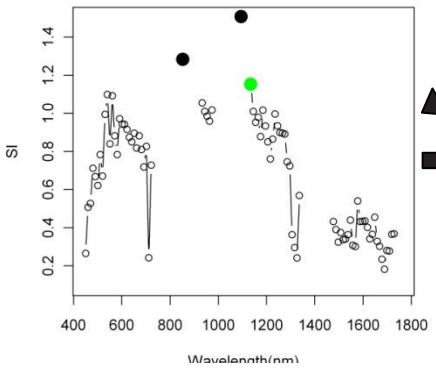

Remove all bands displaying a correlation > c-2i with the selected band (-). Correlation threshold systematically decreases by 0.01.

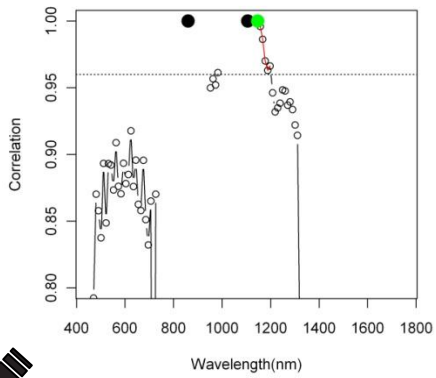

the process continues until no additional bands can be selected

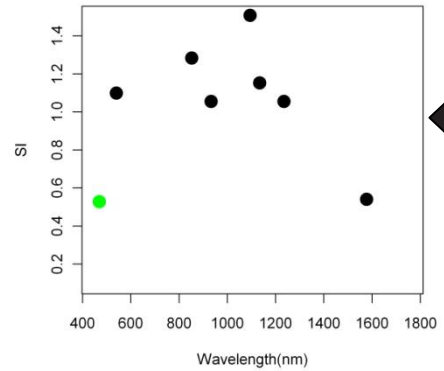

Figure 3 – Schematic overview of the uSZU band selection protocol.

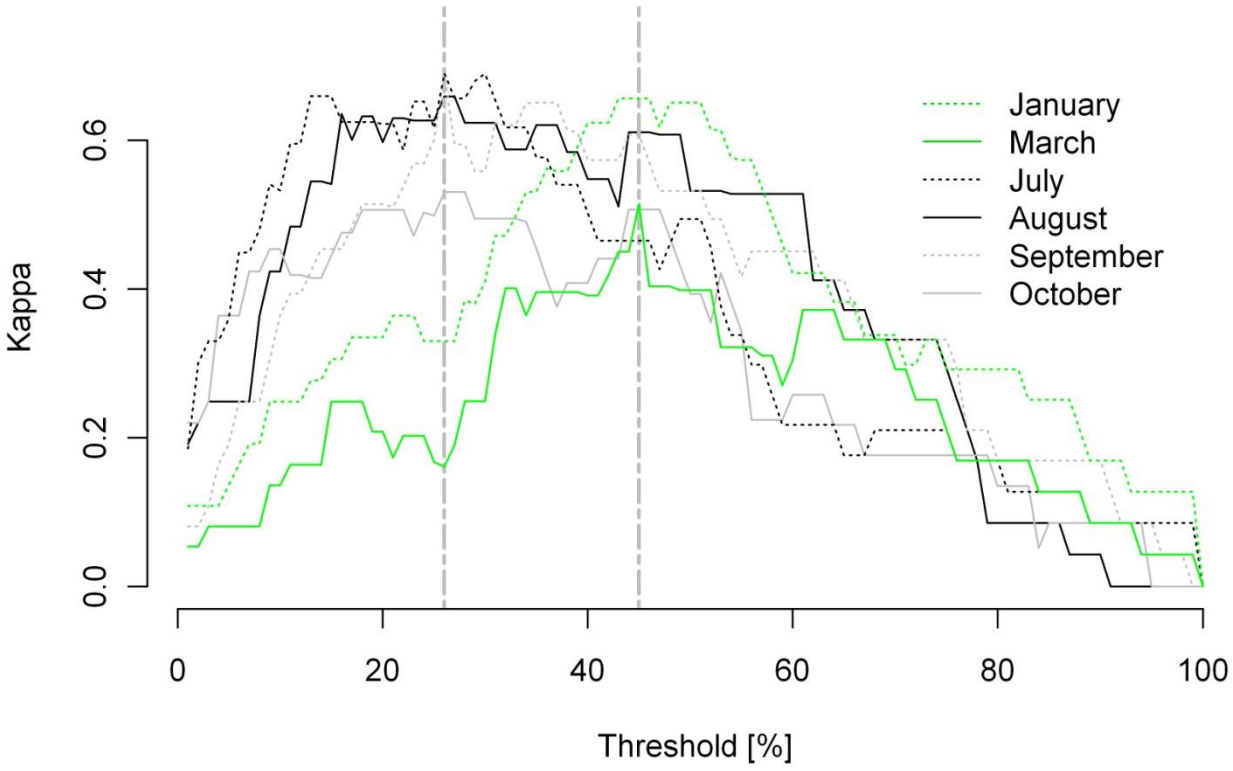

Figure 4 – The seasonal trends in the success of detecting *Morella* invasion, expressed as the Kappa coefficient, as a function of the MESMA classification threshold, are shown for each month. The vertical dotted lines indicate the maximum Kappa values for thresholds of 45% (obtained in January/March) and 25% (obtained in July/August/September/October; adapted from Somers & Asner, 2012a).

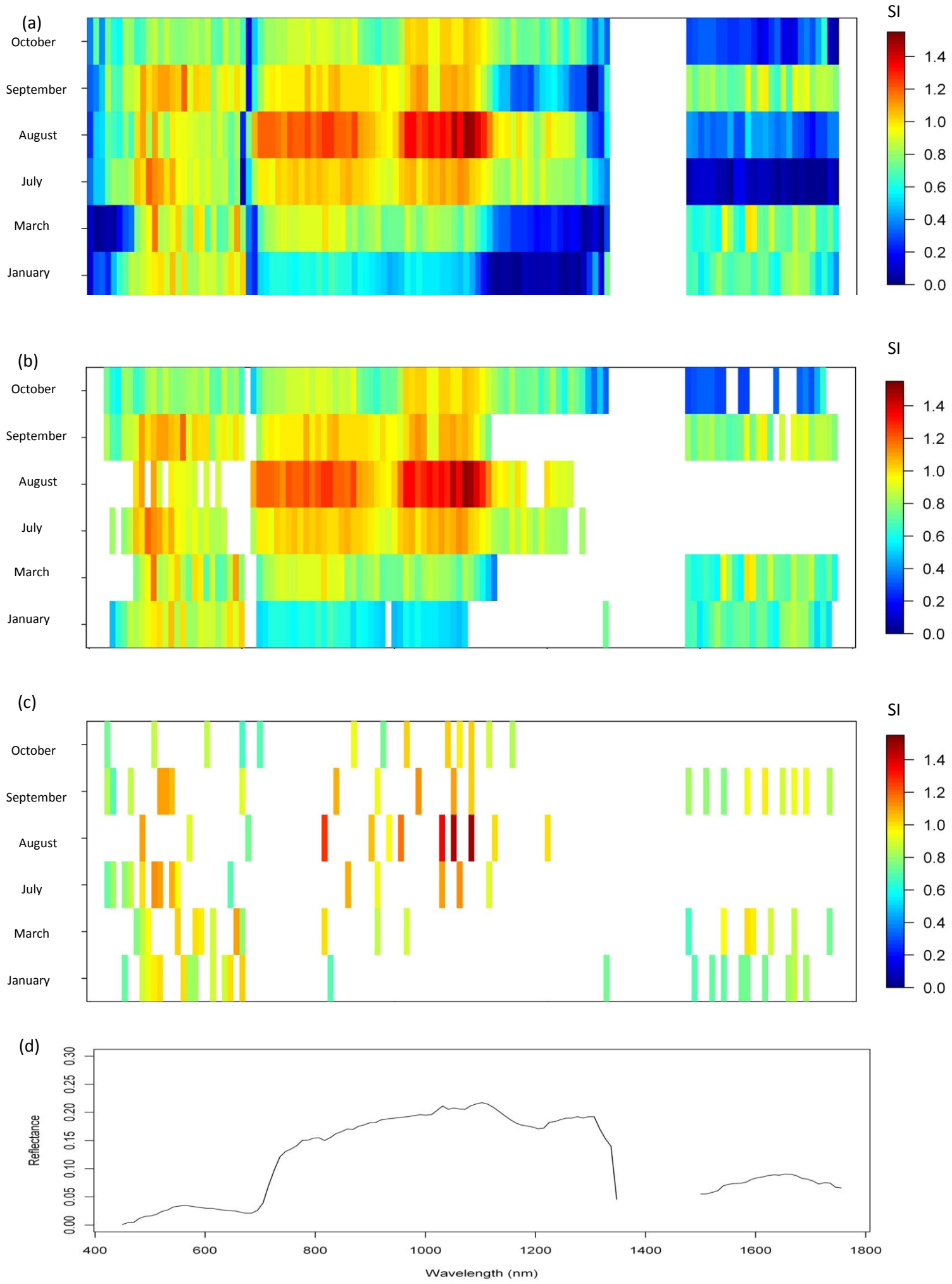

Figure 5 – Spectro-temporal SI charts for the unitemporal implementation of (a) traditional MESMA including all 117 bands per image, (b) SZU and (c) $uSZU_{0.005}$. Panel (d) shows a random vegetation spectrum. The X and Y axis of the different SI charts represent the spectral bands and the time scale respectively.

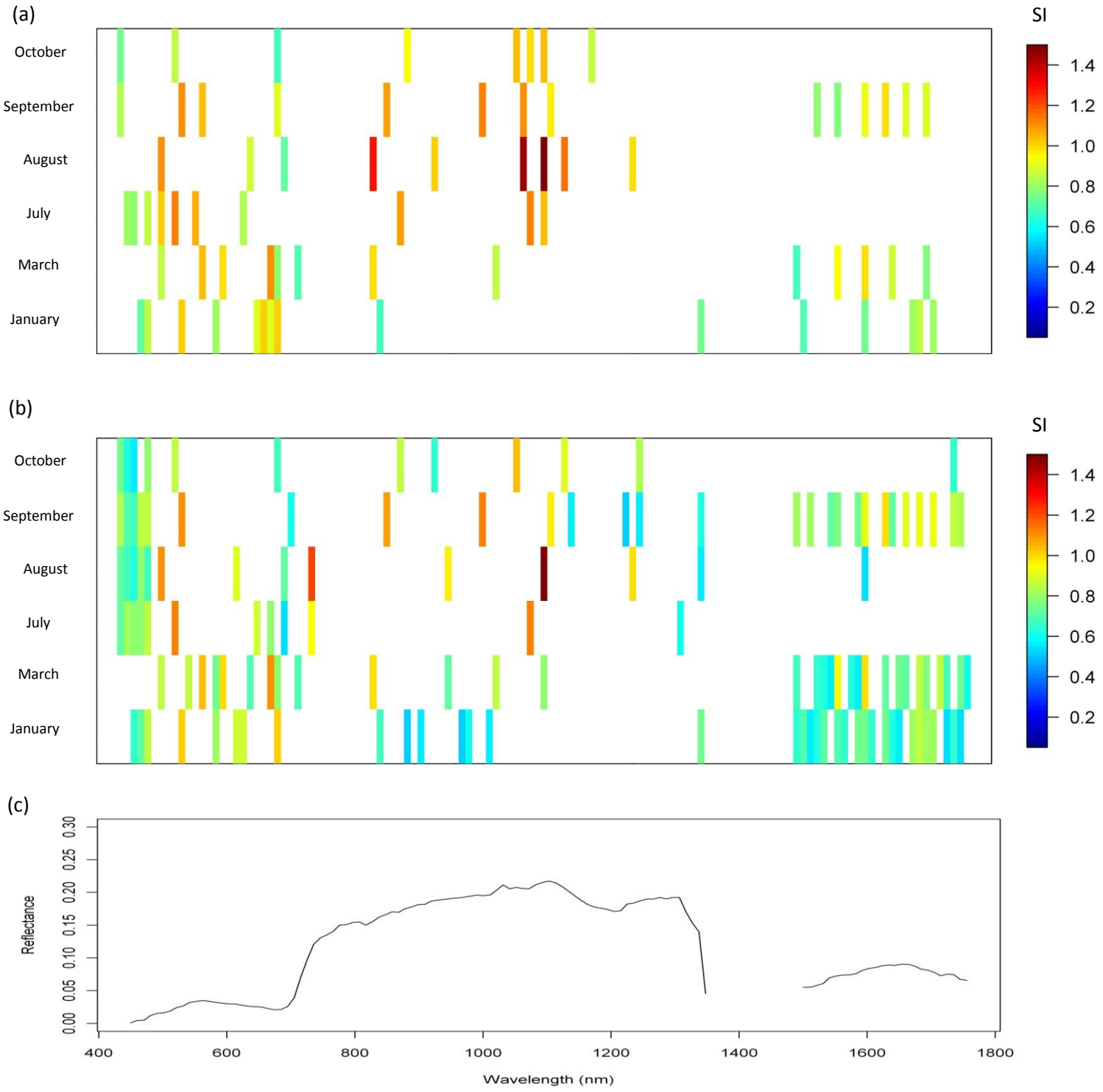

Figure 6 – Spectro-temporal SI charts for the unitemporal implementation of (a) $uSZU_{0.01}$ and (b) $uSZU_{fixed}$. The latter is the uSZU algorithm in which the correlation threshold is fixed to 0.96. This as opposed to a progressively decreasing threshold in uSZU. Panel (d) shows a random vegetation spectrum. The X and Y axis of the different SI charts represent the spectral bands and the time scale respectively.

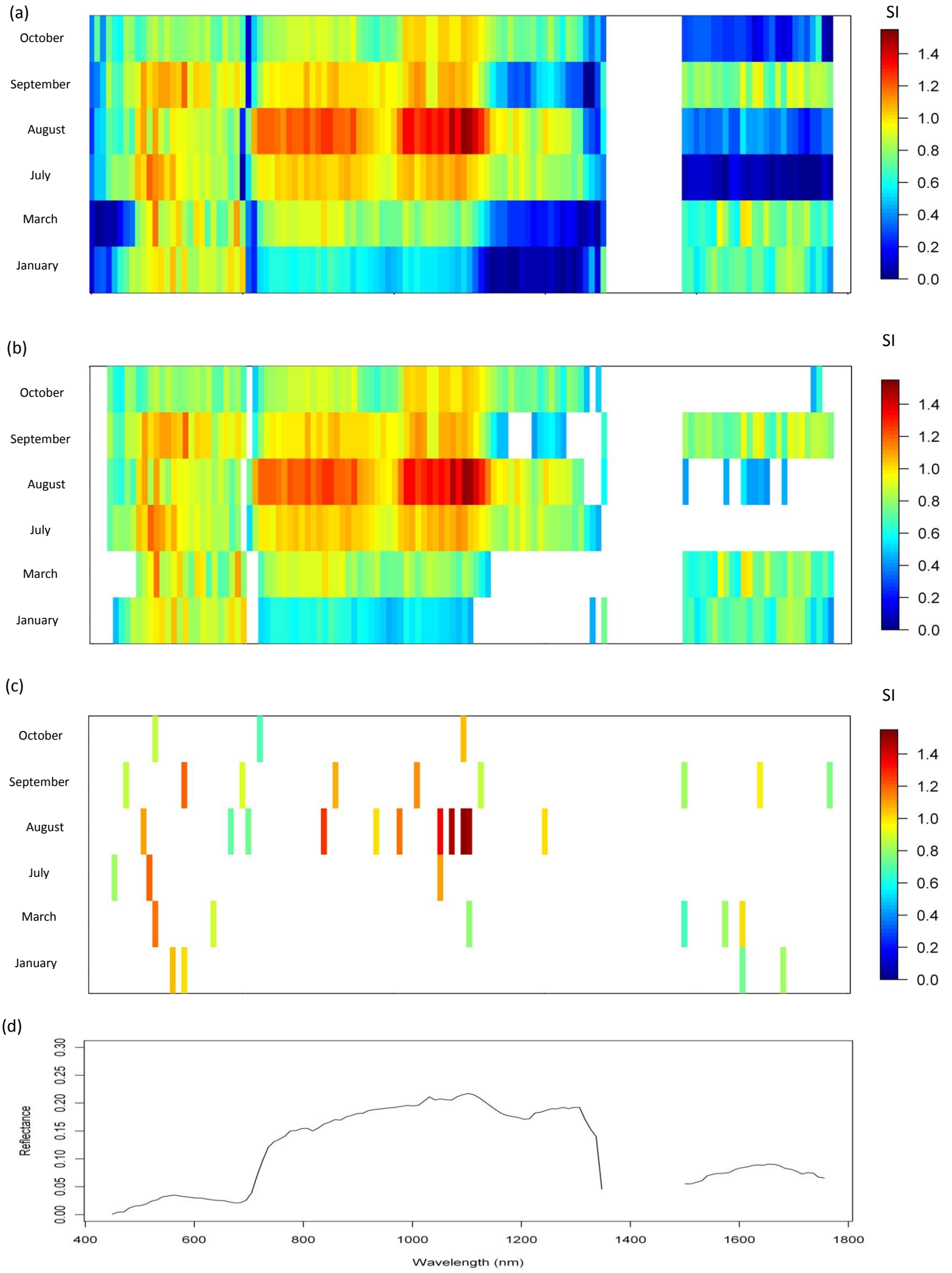

Figure 7 – Spectro-temporal SI charts for the multi-temporal implementation of (a) MESMA, (b) SZU and (c) $uSZU_{0.005}$. Panel (d) shows a random vegetation spectrum. The X and Y axis of the different SI charts represent the spectral bands and the time scale respectively.

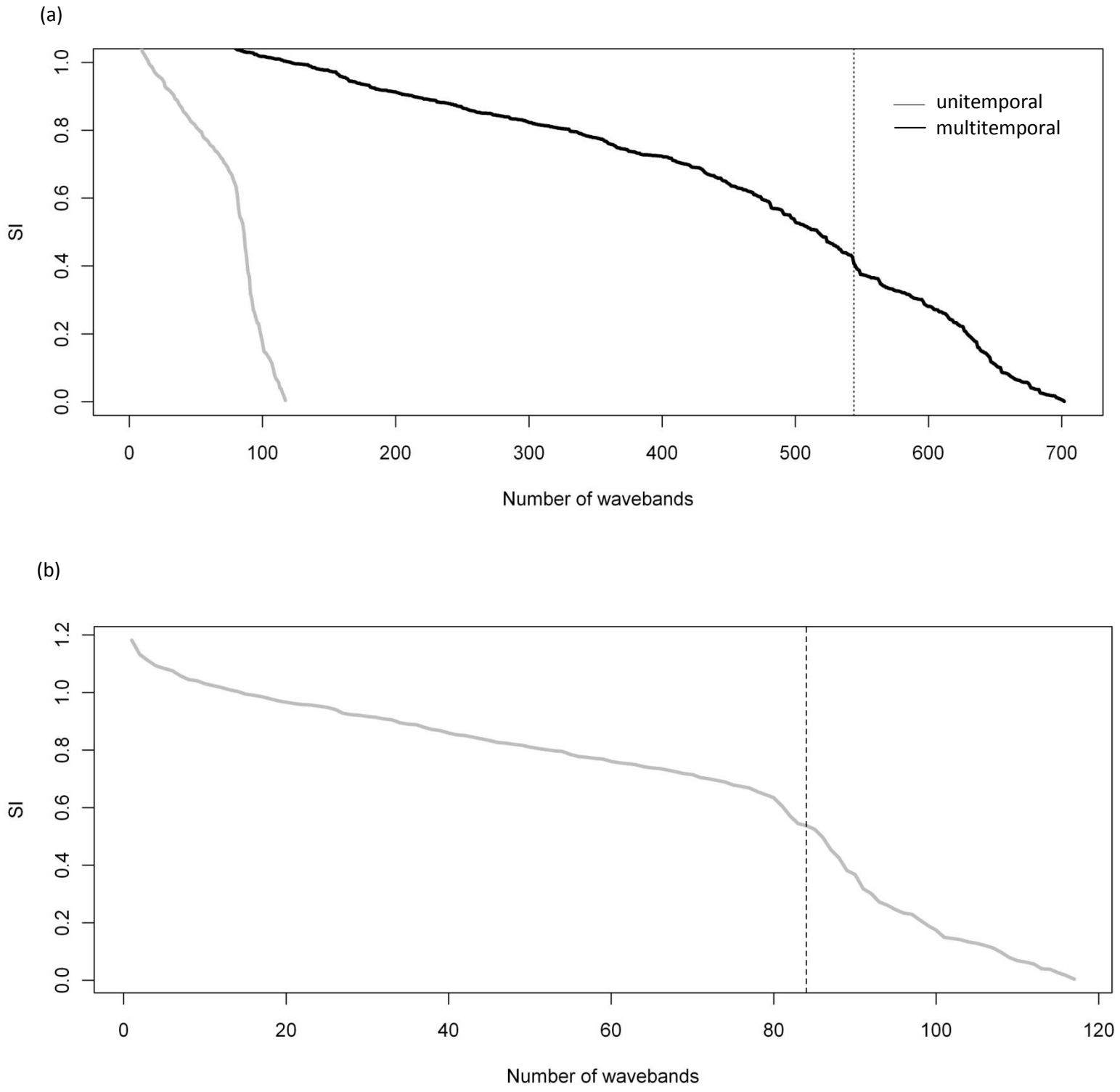

Figure 8 – The band selection protocol of SZU is driven by the relative change in SI between consecutive wavebands (when ordered according decreasing SI, i.e. d_{ISI}, 2.4.1.). In (a) the average decrease in SI for all individual images (unitemporal) with increasing band numbers is compared to the decrease in SI for the temporal composite, containing the spectral information of all six available bands (multitemporal). Due to the gradual decrease in SI as much as 544 wavebands (indicated by the vertical dotted line) were selected by multi-temporal SZU. In the unitemporal approach, for which a detail is shown in (b), 84 bands were selected corresponding to the clear drop in the SI profile (indicated by the vertical dotted line).